Synthesis of a Homologous Series of Ketomethylene Arginyl Pseudodipeptides and Application to Low Molecular Weight Hirudin-like Thrombin Inhibitors†

John DiMaio,* Bernard Gibbs, Jean Lefebvre, Yasuo Konishi, Debra Munn, and Shi Yi Yue

The National Research Council of Canada, Biotechnology Research Institute, 6100, Royalmount Avenue, Montreal, Quebec, Canada, H4P 2R2

Wilfried Hornberger

Knoll AG, Department of Angiology, Ludwigshafen D-6700, Germany. *Received January 17, 1992*

The design of low molecular weight thrombin inhibitors IIa–d (hirutonins) that bind concurrently with the enzyme's catalytic site and auxiliary "anion-binding exosite" for fibrinogen recognition is reported. A practical synthesis of the required homologous ketomethylene arginyl dipeptide inserts [ArgψCO$(CH_2)_n$CO] (n = 1–4) corresponding to the P_1–P_1' scissile position of hirutonins is described. The substitution of the scissile amide function by a ketomethylene group is compatible with the enzyme active site and conferred complete plasma proteolytic stability. This modification also enhanced enzyme affinity up to 20-fold with hirutonin-4 (IIb, n = 4) displaying highest affinity (K_i = 140 ± 20 pM). Hirutonins 1–4 exhibited potent inhibition of plasma prothrombin time (PT) and activated partial thromboplastin time (aPTT). The inhibition was biphasic and showed good correlation with the corresponding K_i. Hirutonin-2 inhibited thrombin-mediated platelet aggregation and exhibited a strong antithrombotic effect comparable to r-hirudin in an in vivo rat arteriovenous shunt model (ED_{15} = 1.20 mg/kg for hirutonin-2 and 1.14 mg/kg for r-hirudin). Lower molecular weight inhibitors were obtained by substituting the six native amino acid residues (Q-S-H-N-D-G), connecting the active site and the auxiliary exosite binding elements with a variable number of intervening ω-aminopentenoyl units. In addition, the exosite component was reduced to seven amino acid residues (D-F-E-P-I-P-L). Incorporation of these modifications into the bifunctional format resulted in nanomolar thrombin inhibitory peptides (IIIa–c). The resulting inhibitors were studied by molecular modeling with α-thrombin, and the bimolecular interactions served to explain the retention of high enzyme affinity.

Introduction

Plasma proteins participating in hemostatis have been implicated in increased risk of cardiovascular disease and indications of thrombosis.[1] The blood coagulation cascade which is bias toward negative regulation, responds rapidly to vascular aberrations by forming a hemostatic plug through recruitment of platelets and formation of a fibrin clot.[2] Therefore, imbalances in this pathway contribute to the formation of thrombi in major arteries and precipitate incidence of myocardial infarction, ischemia, and stroke.[1,3,4]

The enzyme, thrombin, plays a critical role in thrombus formation[6,7] since it converts fibrinogen to fibrin monomer and activates platelets by interacting with a specific platelet membrane receptor.[5,8,9] The enzyme also mediates feedback amplification of its action through activation of the required cofactors V and VIII, as well as the fibrin transpeptidase factor XIIIa.[10] These functions, together with the inflammatory effects on endothelial cells,[11] make thrombin a viable target for therapeutic intervention.

We and others have independently reported highly potent inhibitors of the enzyme thrombin.[12–17] These compounds are structurally related to the COOH terminal tail of the leech anticoagulant protein hirudin,[18,19] but have substantially reduced molecular weight and are modified to preserve the general mechanism, although not the form by which the native protein binds to the enzyme, as observed in the X-ray crystal structure of the bimolecular complex between hirudin and α-thrombin.[20–22] Accordingly, the high potency and specificity of the synthetic inhibitors are secured by the simultaneous occupancy of the enzyme's active site and "anion-binding exosite for fibrinogen recognition" (hereafter referred to as "anion-binding exosite") which is unique to thrombin.[23] In contrast to hirudin, the tripeptidyl component interacting with the catalytic site binds in a substrate-like manner thereby generating a scissile bond which, in the original series (I, Figure 1), was shown to be hydrolyzed[12] in keeping with only partial proteolytic resistance accorded by the imino acid proline as the P_1' residue in substrates of serine

†Contribution No. 33698 from the National Research Council of Canada.

(1) Cook, N. S.; Ubben, D. Fibrinogen as a Major Risk Factor in Cardiovascular Disease. *Trends Pharmacol. Sci.* **1990**, *11*, 444–451.
(2) Mann, K. G.; Jenney, R. J.; Krishnaswamy, S. Cofactor Proteins in the Assembly and Expression of Blood Clotting Enzyme Complexes. *Annu. Rev. Biochem.* **1988**, *57*, 915–956.
(3) Shepard, L. Y. The competitive market for antiplatelets and thrombolytics: can a new entrant succeed. *Trends Biotechnol.* **1991**, *11*, 80–85.
(4) Van De Werf, F. L'Infarctus du Myocarde et la Thrombolyse. *Recherche* **1991**, *22*, 425–433.
(5) Tollefsen, D. M.; Feagler, J. R.; Majerus, P. W. The Binding of Thrombin to the Surface of Human Platelets. *J. Biol. Chem.* **1974**, *249*, 2646–2651.
(6) Hanson, S. R.; Harker, L. A. Interruption of acute platelet-dependent thrombosis by the synthetic antithrombin-D-phenylalanyl-L-prolyl-L-arginylchloromethyl ketone. *Proc. Natl. Acad. Sci. U.S.A.* **1988**, *85*, 3184–3188.
(7) Fitzgerald, D. J.; FitzGerald, G. A. Role of thrombin and thromboxane A_2 in reocclusion following coronary thrombolysis with tissue-type plasminogen activator. *Proc. Natl. Acad. Sci. U.S.A.* **1989**, *86*, 7585–7589.
(8) Harmon, J. T.; Jamieson, G. A. The Glycocalicin Portion of Platelet Glycoprotein Ib Expresses both High and Moderate Affinity Receptor Sites for Thrombin. *J. Biol. Chem.* **1986**, *261*, 15928–15933.
(9) Vu, T.-K.; Hung, D. T.; Wheaton, V. I.; Coughlin, S. R. Molecular Cloning of a Functional Thrombin Receptor Reveals a Novel Proteolytic Mechanism of Receptor Activation. *Cell* **1991**, *64*, 1057–1068.
(10) Walz, D. A., Fenton, J. W., II, Shuman, M. A., Eds. *Bioregulatory Functions of Thrombin*; New York Acad. Sci.: New York, 1986; Vol. 485.
(11) Prescott, S. M.; Seeger, A. R.; Zimmerman, G. A.; McIntyre, T. M.; Maraganore, J. M. Hirudin-based Peptides Block the Inflammatory Effects of Thrombin on Endothelial Cells. *J. Biol. Chem.* **1990**, *265*, 9614–9616.
(12) DiMaio, J.; Gibbs, B.; Munn, D.; Lefebvre, J.; Ni, F.; Konishi, Y. Bifunctional Thrombin Inhibitors Based on the Sequence of Hirudin$^{45-65}$. *J. Biol. Chem.* **1990**, *265*, 21698–21703.
(13) DiMaio, J.; Gibbs, B.; Munn, D.; Lefebvre, J.; Ni, F.; Konishi, Y. Design of Bifunctional Thrombin Inhibitors Based on the Sequence of Hirudin$^{45-65}$. In *Peptides: Proceedings of the 21st European Peptide Symposium*; Giralt, E., Giralt Andreu, D., Eds.; 1990; 774–776.

0022-2623/92/1835-3331$03.00/0

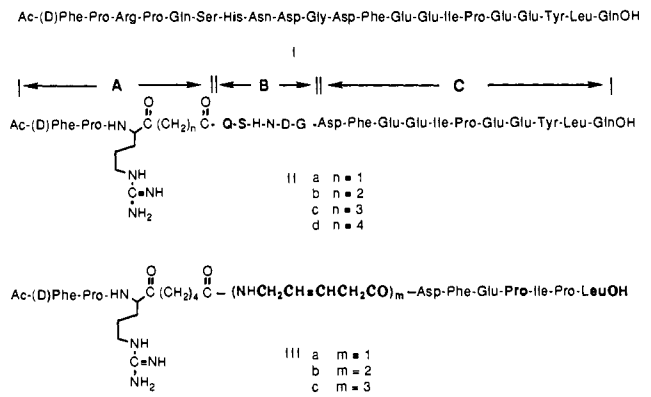

Figure 1. Structure of [Ac-(D)Phe[45],Arg[47]]hirudin45–65 (I), hirutonin 1–4 (IIa–d), and modified hirutonin 4 (IIIa–c).

proteases. We subsequently showed that the insertion of a ketomethylene pseudopeptide (IIb, Figure 1), which is structurally analogous to the scissile position of the natural substrate fibrinogen, conferred higher affinity (K_i = 0.37 ± 0.03 nM) and proteolytic resistance toward thrombin, compared to I.[14] This peptide (hirutonin-2) was designated a bifunctional thrombin inhibitor, because it incorporates the recognition elements of the enzyme's catalytic site (A) and the "anion-binding exosite" (C) which are separated by a third component (B) consisting of amino acid residues 49–54 of the native protein.

We have now identified the minimum structural requirements of the "anion-binding exosite" and the length of a synthetic spacer necessary to bridge this site to the enzyme's catalytic site. In this communication we describe the synthesis of the homologous ketomethylene inserts corresponding to positions 47–48 of inhibitors IIa–d. We also describe molecular modeling studies with hirutonin-2 and its lower molecular weight congeners IIIa–c. The latter incorporate in a bifunctional format a modified truncated exosite sequence, multiple units of a rigid synthetic spacer

Scheme I.[a] Synthesis of Homologous Ketomethylene Inserts for IIb–d

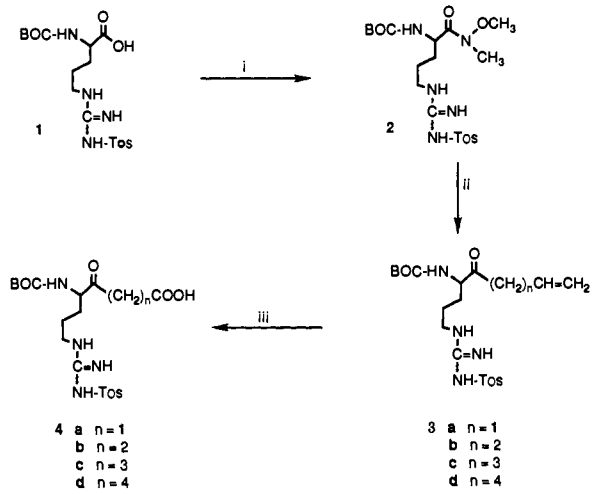

[a] Reagents: (i) $CH_3NH(OCH_3)$, HCl, BOP, DMF, 0 °C; (ii) $MgBr(CH_2)_nCH{=}CH_2$/EtO in THF; (iii) $RhCl_3/NaIO_4$, ACN/H_2O.

Scheme II.[a] Synthesis of N^{α}-Boc Guanidino Norstatone Insert for IIa

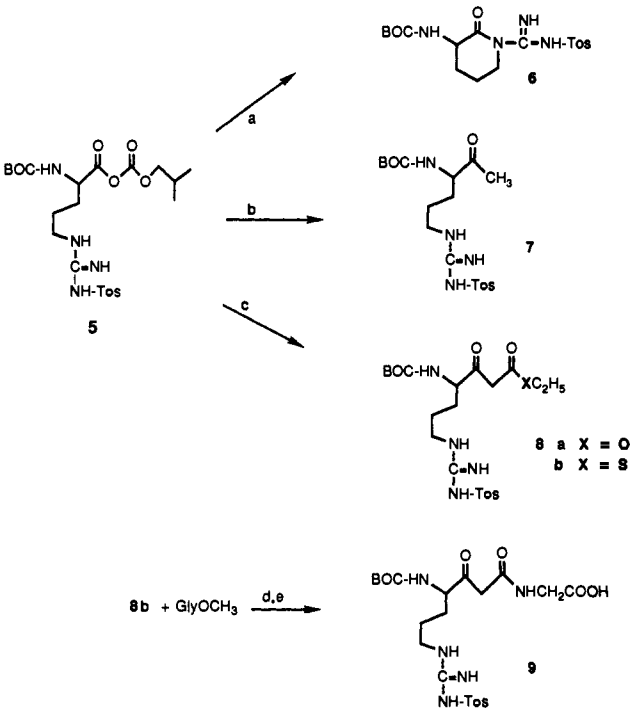

[a] Reagents: (a) *n*-butyllithium/EtOAc/THF; (b) *n*-butyllithium/trimethylsilyl acetate/$ZnCl_2$; (c) *n*-butyllithium/EtOAc or EtSAc/$ZnCl_2$/ether; (d) 8b/CuI/TEA/CH_2Cl_2; (e) NaOH.

and the optimum peptidomimetic moiety for the scissile bond.

Chemistry

Synthesis of Arginyl Dipeptide Inserts. The preparation of the oxo guanidino amino acid inserts required for the synthesis of IIb–d is shown in Scheme I. Ketomethylene surrogates used to stabilize proteolytically susceptible amide bonds have been previously reported[24–26]

(14) DiMaio, J.; Ni, F.; Gibbs, B.; Konishi, Y. A New Class of Potent Thrombin Inhibitors that Incorporates a Scissile Pseudopeptide Bond. *FEBS Lett.* **1991**, *282*, 47–52.
(15) DiMaio, J.; Gibbs, B.; Konishi, Y.; Lefebvre, J.; Munn, D. Homologation of the P_1' site of hirutonins: A new prototype of thrombin inhibitors. In *Peptides: Proceedings of the 12th American Peptide Symposium*; Smith, J. A., Rivier, J. E., Eds.; 1991, 814–815.
(16) Maraganore, J. M.; Bourdon, P.; Jablonski, J.; Ramachandran, K. L.; Fenton, J. W., II. *Biochemistry* **1990**, *29*, 7095–7101.
(17) Kline, T.; Hammond, C.; Bourdon, P.; Maraganore, J. M. Hirulog Peptides with Scissile Bond Replacements Resistant to Thrombin Cleavage. *Biochem. Biophys. Res. Commun.* **1991**, *177*, 1049–1055.
(18) Markwardt, F. Hirudin as an Inhibitor of Thrombin. *Methods Enzymol.* **1970**, *19*, 924–932.
(19) Tripier, D. Hirudin: A Family of Iso-Proteins, Isolation and Sequence Determination of New Hirudins. *Folia Haematol. (Leipzig)* **1988**, *115*, 30–35.
(20) Grütter, M. G.; Priestle, J. P.; Rahuel, J.; Grossenbacher, H.; Bode, W.; Hofsteenge, J.; Stone, S. R. Crystal structure of the thrombin-hirudin complex: a novel mode of serine protease inhibition. *EMBO J.* **1990**, *9*, 2361–2363.
(21) Rydel, T. J.; Ravichandran, K. G.; Tulinsky, A.; Bode, W.; Huber, R.; Roitsch, C.; Fenton, J. W., II. The Structure of a Complex of Recombinant Hirudin and Human α-Thrombin. *Science* **1990**, *249*, 277–280.
(22) Rydel, T. J.; Tulinsky, A.; Bode, W.; Huber, R. Refined Structure of the Hirudin-Thrombin Complex. *J. Mol. Biol.* **1991**, *221*, 583–601.
(23) Chang, J.-Y. Deciphering the Structural Elements of Hirudin C-Terminal Peptide That Bind to the Fibrinogen Recognition Site of α-Thrombin. *Biochemistry* **1991**, *30*, 6656–6661.
(24) Almquist, R. G.; Chao, W. R.; Ellis, M. E.; Johnson, H. L. Synthesis and Biological Activity of a Ketomethylene Analog of a Tripeptide Inhibitor of Angiotensin Converting Enzyme. *J. Med. Chem.* **1980**, *23*, 1392–1398.

Scheme III.[a] Synthesis of *N*-Boc-5-Amino-3-pentenoic Acid Unit Serving as the Spacer for IIIa–c

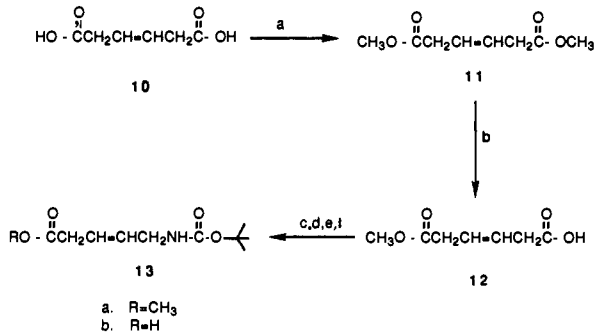

[a] Reagents: (a) EtOH/benzene, TosOH, Δ; (b) pig liver esterase, H_2O, LiOH pH 7.5; (c) $COCl_2$/benzene; (d) $NaN_3/CH_3COCH_3/H_2O$; (e) *tert*-butyl alcohol/toluene, Δ; (f) LiOH or pig liver esterase.

but these methods are not readily applicable to arginine and do not allow access to homologation as required in this study. We turned our attention to the possibility of using the *N,O*-dimethylhydroxamate of N^{α}-Boc-N^{ω}-tosylarginine as an acylating agent as originally described by Nahm and Weinreb[27] and elaborated by Castro.[28] Reaction of **2** with a 10-fold excess of the appropriate Grignard reagent gave the unsaturated ketones **3b–d**. Subsequent Sharpless oxidation[29] of the resulting terminal alkene provided the required homologous acids **4b–d**. Reaction of the Grignard reagent derived from allyl bromide afforded predominantly the conjugated ketone which upon oxidation afforded a complex mixture from which only starting N^{α}-Boc-N^{ω}-tosylarginine could be recovered. Consequently **4a** could not be obtained by this route.

For the synthesis of the guanidino norstatone required for IIa, we then turned to the reported acylation of metal enolates with alkyl and aryl *N,O*-dimethylhydroxamates.[30] No reaction took place between **2** and ethyl lithioacetate whereas application of the same reaction to the mixed anhydride **5** (Scheme II) afforded only the N^{ω}-lactam **6**. This quantitative side reaction was circumvented by trans metalation using $ZnCl_2$ or $MgBr_2 \cdot Et_2O$ in ether prior to the addition of the mixed anhydride. Although this approach provided a good yield of β-keto ester **8a**, the product underwent a retro-Claisen reaction upon saponification with NaOH. Reaction of the mixed anhydride with the Zn enolate of trimethylsilyl acetate was also abortive since workup was accompanied by solvolysis of the trimethylsilyl ester group and decarboxylation affording **7** (path b).

Table I. Inhibitory Dissociation Constants for the Human α-Thrombin-Mediated Hydrolysis of the Fluorescent Substrate Tosyl-Gly-Pro-Arg-Amc

analog	K_i, nM[a]
r-hirudin HV2 (K47)	0.00038 ± 0.00005
hirudin[45–65]	110 ± 3
I	2.8 ± 0.9
IIa	3.8 ± 0.1
IIb	0.37 ± 0.03
IIc	0.56 ± 0.14
IId	0.14 ± 0.02
IIIa	300 ± 20
IIIb	3.5 ± 1.8
IIIc	3.2 ± 1.1

[a] Mean of three determinations ± SEM. Conditions and data analysis are provided in the Experimental Section.

The procedure finally adopted was based on the favorable rates of coupling reaction reported for thioesters and amino acid esters catalyzed by a thiophilic metal contained in CuI.[31] Kim et al.[32] have extended this reaction to β-keto thioesters. Having established a procedure for obtaining the ethyl β-keto ester of N^{α}-Boc-N^{ω}-tosylarginine, the reaction was extended to provide a good yield of the corresponding thioester **8b**. It was envisaged that the β-keto thioester could undergo direct CuI-catalyzed coupling to the protected resin-bound peptide terminating with the required Gln49 residue. However, although model experiments showed that the β-keto thioester underwent rapid CuI-catalyzed coupling with a variety of α-amino acid esters, as well as amino acyl resins (unpublished results), it failed to react with the required peptide resin terminating with Gln. Subsequently it was realized that the reaction of NH_2Gln-OMe and the thioester **8b** under standard conditions also gave only complex product mixtures by HPLC, indicating that the amino acid Gln is problematic in this reaction scheme. Therefore, the model compound **9** was synthesized which effectively replaces the Gln49 position by glycine, a substitution that only moderately affects potency of these bifunctional inhibitors.[33]

Synthesis of the Spacer Unit. (N^{ω}-Boc-amino)-*trans*-3-pentenoic acid (Scheme III) was synthesized by a modified procedure of Cox et al.[34] In our hands the original method using $BF_3 \cdot Et_2O$ in dioxane yielded a mixture of monomethyl, dimethyl, and starting material β-*trans*-hydromuconic acid. Alternatively, the starting material could be exhaustively esterified using methanol and a catalytic amount of *p*-toluenesulfonic acid in benzene at reflux. The product was subjected to enzymatic hydrolysis using pig liver esterase affording a quantitative yield of the monoacid **12**. Attempts to convert the monocarboxylic acid to the [*N*-(*tert*-butyloxycarbonyl)-amino]pentenoic acid ester directly using DPPA resulted in only low product yields (<10%). However, formation of the acid chloride with oxalyl chloride followed by re-

(25) Rich, D. H.; Bopari, A. S.; Bernatowicz, M. S. Synthesis of a 3-oxo-4(S)-amino acid analog of pepstatin. *Biochem. Biophys. Res. Commun.* **1982**, *104*, 1127–1133.

(26) Thaisrivong, S.; Pals, D. T.; Kati, W. M.; Turner, S. R.; Thomasco, L. M.; Watt, W. Design and Synthesis of Potent and Specific Renin Inhibitors Containing Difluorostatine Difluorostatone and Related Analogues. *J. Med. Chem.* **1986**, *29*, 2080–2087.

(27) Nahm, S.; Weinreb, S. M. N-Methoxy-N-Methylamides as Effective Acylating Agents. *Tetrahedron Lett.* **1981**, *22*, 3815–3818.

(28) Fehrentz, Y. A.; Castro, B. An Efficient Synthesis of Optically Active α-(*t*-Butyloxycarbonylamino)-aldehydes from α-Amino Acids. *Synthesis* **1983**, 676–678.

(29) Carlsen, P. H. J.; Katsuki, T.; Martin, V. S.; Sharpless, K. B. A Greatly Improved Procedure for Ruthenium Tetraoxide Catalyzed Oxidation of Organic Compounds. *J. Org. Chem.* **1981**, *46*, 3936–3938.

(30) Turner, J. A.; Jacks, W. S. Acylation of Ester Enolates by N-Methoxy-N-Methylamides: An Effective Synthesis of β-Keto Esters. *J. Org. Chem.* **1989**, *54*, 4229–4231.

(31) Masamune, S.; Kamata, S.; Schilling, W. Syntheses of macrolide antibiotics. III. Direct ester and lactone synthesis from S-*tert*-butyl thioate thiol ester. *J. Am. Chem. Soc.* **1975**, *97*, 3515–3516.

(32) Kim, H.-O.; Olsen, R. K.; Choi, O.-S. Copper(I)-Promoted Condensation of α-Amino Acids with β-Keto Thioesters: Synthesis of N-Acylated L-Leucine Derivatives Containing (*S*)-4-Hydroxy-5-methyl- and (*S*)-4-Hydroxy-2,5-dimethyl-3-oxohexanoic Acid. *J. Org. Chem.* **1987**, *52*, 4531–4536.

(33) Yue, S. Y.; DiMaio, J.; Szewczuk, Z.; Purisima, E. O.; Ni, F.; Konishi, Y. Characterization of the Interactions of a Bifunctional Inhibitor with α-Thrombin by Molecular Modeling and Peptide Synthesis. *Prot. Eng.* **1992**, *5*, 77–85.

(34) Cox, M. T.; Heaton, D. W.; Horbury, J. Preparation of Protected *trans*-Olefinic Dipeptide Isosteres. *J. Chem. Soc. Chem. Commun.* **1980**, 799–800.

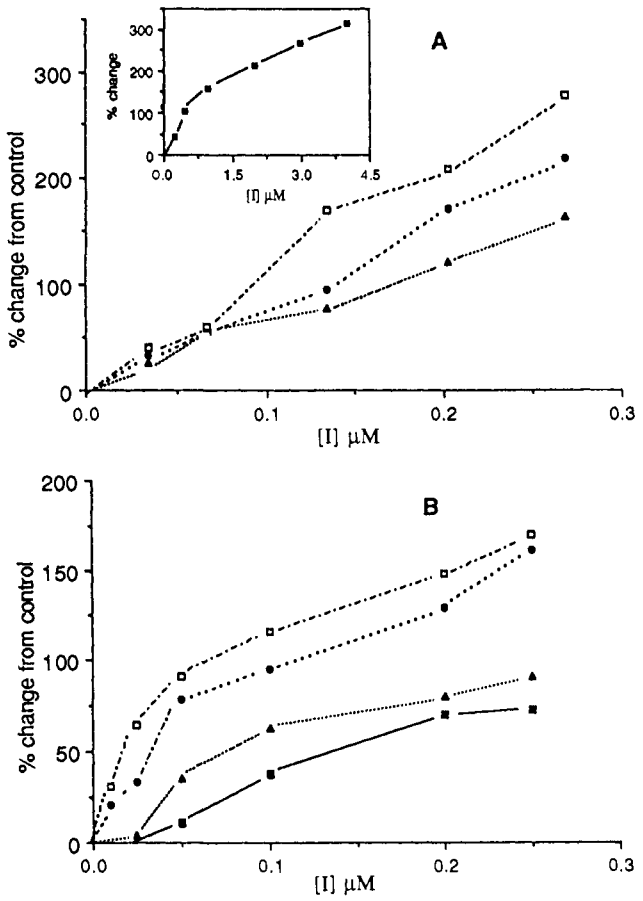

Figure 2. Inhibition of plasma prothrombin time (A) and activated partial thromboplastin time (B) by IIa (—■—), IIb (- - -●- - -), IIc (··· ▲ ···), and IId (- - - □ - - -). Each point is the mean of three determinations.

action with NaN_3 and rearrangement by heating in toluene in the presence of *tert*-butyl alcohol, afforded a 70–80% yield of **13a** which was saponified to the acid **13b** using LiOH or pig liver esterase.

Peptide Synthesis. All the hirudin peptides reported in this paper were synthesized by the solid-phase method on an Applied Biosystems 430A peptide synthesizer. *tert*-(Butyloxycarbonyl)-Gln or -Leu (phenylacetamido)-methyl (PAM) resins were used as the solid-phase support (0.64 mmol/g). All couplings were mediated by dicyclohexylcarbodiimide/*N*-hydroxybenzotriazole, and deprotections were carried out using 50% TFA/CH_2Cl_2. For best results, the terminal D-Phe and Pro residues were incorporated as the dipeptide Boc-(D)Phe-Pro. This strategy avoided the propensity of the penultimate proline residue to undergo intramolecular cyclization with the ketone function of the preceding residue after acid deprotection.

Results

Peptides IIa–d and IIIa–c were evaluated for their ability to inhibit the α-thrombin-mediated hydrolysis of the fluorescent substrate Tos-Gly-Pro-Arg-Amc. The results are shown in Table I. All the compounds were found to be competitive inhibitors of human α-thrombin with hirutonin-4 showing the highest enzyme affinity (K_i = 0.14 ± 0.02 nM). This value represents a 1000-fold improvement over the native C-terminal sequence corresponding to desulfohirudin45–65 which exhibited mixed-type kinetic behavior compared to ketomethylene congeners.[12] With the exception of hirutonin-3, a progressive enhancement in affinity was observed with increasing chain length

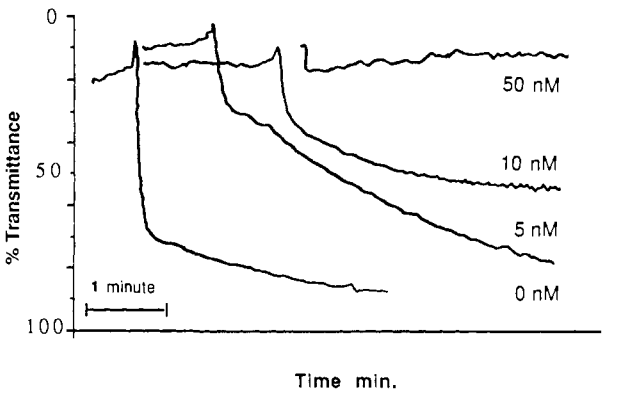

Figure 3. Inhibition of α-thrombin-mediated platelet aggregation by hirutonin-2 (IIb).

Table II. Antithrombotic Effect of IIb (Hirutonin-2) and IIIb Compared to Recombinant Hirudin in the Rat Aretiovenous Shunt Model after Intravenous Administration

compound	ED_{15}, mg/kg[a]	n[b]
r-hirudin	1.42 (1.14–1.92)	24
IIb	1.20 (0.82–2.44)	55
IIIb	6.27 (4.48–11.2)	20

[a] Dose (95% confidence limits) of compound required to produce a 15-min prolongation in shunt patency. [b] n = number of experimental animals.

separating the ketone function and the amide carbonyl linking Gln49. Compared to the bifunctional inhibitors in Table I, the inhibitory dissociation constants of the homologous acetylated tripeptidyl esters corresponding to component A (Figure 1) of hirutonin peptides were invariant (14–18 μM). Hirutonin-1 which has a β-keto amide function in the scissile position, analogous to some statone renin inhibitors,[25] had the lowest affinity among the homologous series. Although this peptide has a Gly49 residue instead of the native Gln49, this substitution alone does not explain the lower affinity since the same replacement in the series prototyped by I was shown to cause less than a 2-fold increase in K_i.[33]

Hirutonins 1–4 showed dose-dependent inhibition of human plasma prothrombin time (PT) and activated partial thromboplastin time (aPTT) (Figure 2). In these clotting assays the synthetic inhibitors exhibited a biphasic anticoagulant response which leveled off, especially in the aPTT assay. The ceiling of anticoagulant activity correlated well with the corresponding K_i values. In both assays the weakest inhibitor was hirutonin-1 (IIa), which at 3 μM prolonged the prothrombin time by 250% from the control (18 s) compared to 800% for its next higher homolog.

Thrombin is a mediator of platelet-dependent formation of a hemostatic plug at the site of tissue damage and is partly responsible for delaying reperfusion and inducing reocclusion following coronary thrombolysis.[6,7] Hirutonin-2 inhibited thrombin-induced platelet aggregation in vitro (Figure 3), but not ADP or epinephrine. Half-maximum inhibition was observed at 10 nM. Preliminary in vivo studies showed that hirutonin-2 possesses potent antithrombotic activity. In the rat arteriovenous shunt model, compound IIb was as potent as *r*-hirudin in prolonging the patency of the shunt (Table II), despite the drastically reduced size.

The plasma proteolytic stability of hirutonin-2 was also evaluated. Figure 4 shows that compared to I, hirutonin-2 is proteolytically stable toward plasma proteases after 30 min. The primary degradation product of peptide I results from the proteolysis of the P_1–P_1' scissile bond as evidenced by the appearance of a new peak at 22 min (Figure

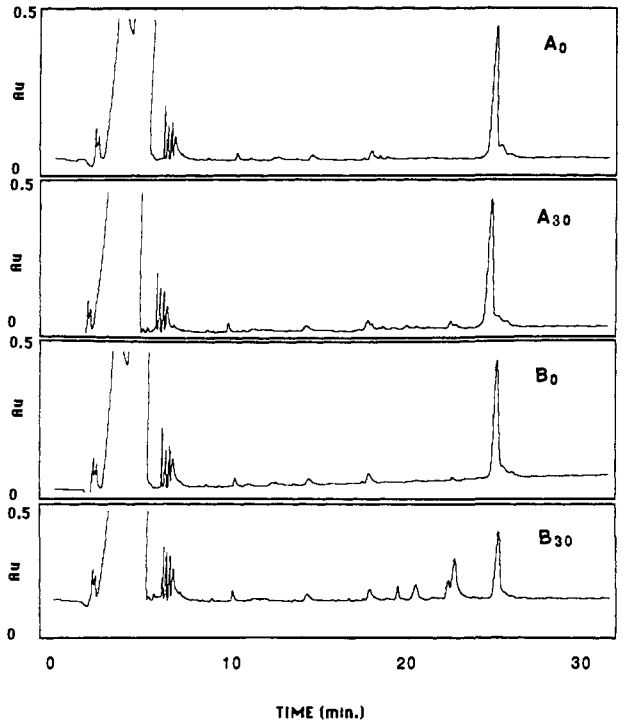

Figure 4. Comparative in vitro plasma proteolytic stability of IIb (A) and I (B). HPLC spectra were recorded at zero time (A_0 and B_0) and after 30-min incubation (A_{30} and B_{30}).

4B) corresponding to the fragment hirudin48–65. By comparison, the ketomethylene function in IIb confers complete resistance (Figure 4A). One minor metabolite observed after 2 h was the result of proteolysis between Glu61 and Glu62 analogous to native hirudin.[37]

Peptides IIIa–c differ from the series IIa–d in three ways (Figure 1): Firstly, residues Gln-Ser-His-Asn-Asp-Gly corresponding to the sequence separating the respective active site and anion binding exosite-directed components were removed and replaced by one or multiple ω-aminopentenoyl units. Secondly, the complementary anion-binding exosite sequence Asp55–Gln65 was truncated internally, while retaining the leucine residue. This manipulation has been shown to only modestly affect antithrombin activity.[33] Thirdly, the Glu58 residue of the truncated exosite inhibitor component was mutated to proline (E58P) since this substitution is found in the native sequence of a hirudin variant[35] (hirudin-PA) and has been shown to enhance antithrombin activity.[36] The combination of these modifications and inclusion of the insert for IId, afforded inhibitors with only a 20-fold increase in K_i when $m = 2$ or 3 (Table I), but 2000-fold reduced affinity when $m = 1$. Compared to hirutonin-2, hirudin peptide IIIb showed only 5-fold reduced activity in vivo.

Using model hirutonin peptides IIb and IIIb, the selectivity for the active site of thrombin was investigated using tripeptidyl substrates for trypsin, chymotrypsin, plasmin, and factor Xa. At concentrations up to 10 μM, neither of these hirutonin peptides inhibited any of these proteases.

(35) Dodt, J.; Seemuller, U.; Fritz, H.; Fink, E. Ger. Offen. DE3445532, 1986.

(36) Krtenansky, J. L.; Broersma, R. J.; Owen, T. J.; Payne, M. H.; Yates, M.; Mao, S. J. T. Development of MDL 28,050, a Small Stable Antithrombin Agent Based on a Functional Domain of the Leech Protein, Hirudin. *Thromb. Haemostasis* **1990**, *63*, 208–214.

(37) Chang, J.-Y. The functional domain of hirudin, a thrombin-specific inhibitor. *FEBS Lett.* **1983**, *164*, 307–313.

Molecular Modeling and Discussion

In a previous publication, the modeling of hirudin peptide I complexed with α-thrombin B-chain was described.[33] In the present study the molecular modeling experiments were extended to hirutonin peptides IIa–d and IIIa–c in an effort to correlate biological activity with possible bimolecular interactions.

Figure 5a shows a stereoview of a low-energy conformer of I, IIb, and IIIb docked onto the thrombin catalytic site and extending into the S′ groove of the enzyme. A priori we cannot account for the enhanced enzyme affinity of IIb (compared to I) on stereoelectronic grounds since the respective arginyl carbonyl functions have the same orientation and the catalytic Ser195 residue is 3 Å away from the carbonyl carbon of IIb thereby unlikely to form a hemiketal similar to PPACK thrombin.[38] On the other hand the computed models reveal that hirutonin-2, or its congeners in the series IIa–d, do not bind to thrombin in a substrate-like manner beyond S_1–S_1'; instead the backbone of residues Gln49–Ser50 exits from the deep active site cleft. This property could be an important conformational requirement that may be more compatible with the enhanced flexibility of Argψ($COCH_2$)CH_2CO compared to Arg-Pro in the active site cleft which is narrowed by the thrombin insertion loop between L60–E61.[38]

Residues Gln49–Ser50 are followed by the sequence His-Asn-Asp-Gly whose backbone projects above the enzyme surface with the side chains of Gln49, Asn52, and Asp53 exposed to solvent. These combined amino side chains do not appear to contribute any apparent binding interactions with this region of the enzyme. Accordingly, it was shown that singular substitution of each residue in this region by glycine only marginally affected enzyme affinity.[33] In addition, Maraganore et al. have reported that in related hirulogs, a tetraglycine spacer coupled to an exosite component consisting of residues Asn53–Leu64 is compatible with efficient enzyme interaction.[16] Given the above considerations, variable units of the Glyψ-[CH=CH]Gly dipeptidyl surrogate were substituted for the intervening residues Q-S-H-N-D-G. The results in Table I demonstrate that high potency is retained in the second series (IIIa–c) whose sequence Q-S-H-N-D-G is replaced by multiple ω-aminopentenoyl units devoid of side chain. Figure 5a shows a low-energy conformer of the spacer component of IIIb ($m = 2$) connected through a ketobutylene as the P_1' subsite. As is the case for IIb, the ketobutylene chain of IIIb also emerges from the deep active site cleft but, because of its increased length, extends beyond S_1' and could contribute additional hydrophobic interactions with Trp60D. In contrast to the native backbone conformation of IIb, the two-Glyψ[CH=CH]Gly IIIb are in a fully extended conformation and remain deeper within the thrombin S′ groove. Since a single ω-aminopentenoyl unit would not be expected to effectively span the equivalent distance, the low K_i value for the congener IIIa is anomalous. However, it is likely that a frame shift in the auxiliary anion-binding site could force Asp55 and Phe56 outside of the exosite and function as "spacer" residues. Alternatively, the synthetic spacer may be involved in bimolecular interactions within the S′ groove that would otherwise be inaccessible to the native amino acid sequence, and which would not necessitate interaction with the exosite.

(38) Bode, W.; Mayr, I.; Baumann, U.; Huber, R.; Stone, S. R.; Hofsteenge, J. The refined 1.9 Å crystal structure of human α-thrombin: interaction with D-Phe-Pro-Arg-chloromethylketone and significance of the Tyr-Pro-Pro-Trp insertion segment. *EMBO J.* **1989**, *8*, 3467–3475.

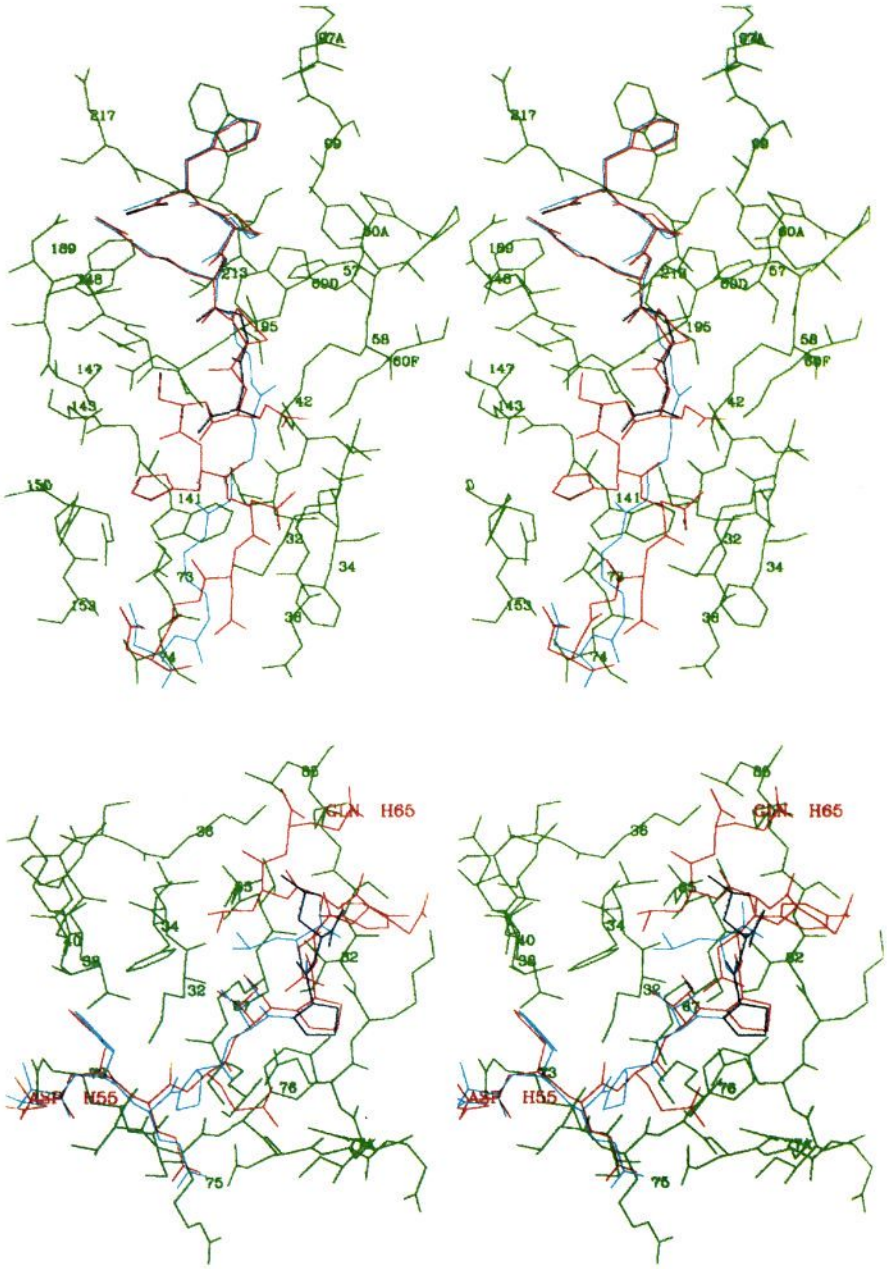

Figure 5. (a, top) Stereo trace of the superimposition of a low energy conformer of I (red), IIb (black) and IIIb (blue) in the primary active site and within the S_1' groove of thrombin. Enzyme residues are numbered. (b, bottom) Superimposed stereoview of the full length fragment 55–65 of IIb (red) and modified truncated exosite component of IIIb. In the blue trace the isobutyl side chain of Leu61 in IIIb is in the *inside* low energy conformation and almost coincident with the same moiety in the full length congener. In the *extended* conformation (black) the isobutyl side chain does not share this property but still interacts with Leu65 and Ile82 of thrombin.

The thrombin "anion-binding exosite" is an auxiliary binding site unique to that enzyme. This site accomodates a variety of either substrates or inhibitors including fibrinogen, the extracellular domain of the thrombin platelet receptor,[39,40] thrombomodulin,[41] and hirudin.[20-22] The interaction of hirudin with the enzyme's exosite has been investigated by NMR[42] and X-ray crystallography. The residues Phe56, Ile59, and Leu64, whose side chain resides proximal to Ile59 through a 3_{10} helical reverse turn, form a contiguous hydrophobic surface that binds to two complementary hydrophobic surfaces on the enzyme[33] (Figure 5b, green). The removal of Gln65 and deletion of internal residues Glu61, Glu62, and Tyr63 from hirudin55–65 places leucine adjacent to Pro60. We have already shown that this operation caused only a modest 30-fold drop in the inhibition of thrombin fibrinogenolytic activity,[33] which could be enhanced 2-fold with the substitution E58P (IC_{50} = 25 μM). Table I shows that the incorporation of the

(39) Liu, L.-W.; Vu, T.-K. H.; Esmon, C. T.; Coughlin, S. R. The Region of the Thrombin Receptor Resembling Hirudin Binds to Thrombin and Alters Enzyme Specificity. *J. Biol. Chem.* **1991**, *266*, 16977–16980.

(40) Vu, T.-K. H.; Wheaton, V. I.; Hung, D. T.; Charo, I.; Coughlin, S. R. *Nature* **1991**, *353*, 674–677.

(41) Suzuki, K.; Nishioka, J.; Hayashi, T. Localization of Thrombomodulin-binding site Within Human Thrombin. *J. Biol. Chem.* **1990**, *265*, 13263–13267.

(42) Ni, F.; Konishi, Y.; Scheraga, H. A. Thrombin-Bound Conformation of the C-Terminal Fragments of Hirudin Determined by Transferred Nuclear Overhauser Effects. *Biochemistry* **1990**, *29*, 4479–4489.

resulting truncated exosite-directed peptide D-F-E-P-I-P-L into a bifunctional format using multiple Glyψ[CH=CH]Gly intervening units resulted in retention of high enzyme affinity (K_i = 3.5 nM, m = 2).

In order to acquire an insight into probable molecular interactions responsible for the high potency of hirutonins IIIb and IIIc, a conformational search was performed using the truncated peptide D-F-E-P-I-P-L. The conformational search found 160 low-energy conformers within the energy window (see Experimental Section). These conformers were grouped into two populations that could be distinguished on the basis of the orientation of the Leu61 side chain of the inhibitor. On the one hand, the side chain projected toward the top rim of the enzyme's exosite (*inside conformer*) with Pro60 ψ = 117°, Leu61 φ = −94°, and Leu61 χ_1 = −66° corresponding to the lowest energy conformer. On the other, an equally populated group had the same side chain projecting onto the surface of the lower bottom (*extended conformer*) with Pro60 ψ = 147°, Leu61 φ = −171°, and Leu61 χ_1 = −155° as the lowest energy conformer. The energy difference between the two was 13 kcal/mol, with the latter being the more stable conformer. For comparison, Figure 5b shows a superposition of the acetylated native inhibitor fragment 55–65 and its truncated counterpart shown in blue (*inside conformer*) and black (*extended conformer*). Noteworthy is that in the former the leucine side chain of the truncated and full length peptide are almost coincident and in hydrophobic contact with Leu65, Ile82 of thrombin, and also Ile59 of the inhibitor. The orientation of the Leu61 side chain in the *extended* conformer also permits favorable interaction with the same enzyme residues, but not with Ile59 of inhibitor.

Although the lowest energy conformers in the eight Monte Carlo searches had an *extended* Leu61, the difference in energies in both populations was not large enough to suggest a single conformation for the bound inhibitor. Further, since the proportion of *inside* versus *extended* conformers was almost 1:1, both were used in subsequent molecular dynamics simulation to study the conformational stability of the respective leucine side chains. The results of the dynamics simulations did not indicate any interconversion between the Leu61 *inside* to Leu61 *extended* conformers. Instead, after 150-ps dynamics simulation, the Leu61 side chain of the *extended* lowest energy conformer consistently rearranged into an intermediate position exposed to solvent having no hydrophobic contacts (dynamics average, Pro60 ψ = 169°, Leu61 φ = −90° and Leu61 χ_1 = −70°). However, the critical hydrophobic cluster involving inhibitor residues (Leu61 and Ile59) and enzyme residues (Leu65 and Ile82) remained with the *inside* conformation (dynamics average, Pro60 ψ = 127°, Leu61 φ = −101° and Leu61 χ_1 = −69°) as observed in the original conformational search (Figure 5b). Therefore, the above results suggest that the truncation and concomitant transposition of the leucine residue may have had an effect which conserves the overall hydrophobic cluster characteristic of the native molecule. Alternatively, the leucine side chain may have uncovered another hydrophobic, albeit unstable, interaction which is not accessible to the native glutamic acid residue in the same position. These possibilities provide venues for modification in order to further reduce the size and enhance activity of these hirutonin peptides.

Conclusion

In this paper, we have described the synthesis and molecular modeling of low molecular weight thrombin inhibitors that simulate the hirudin–thrombin interaction by occupying two independent sites on the enzyme simultaneously. A practical synthesis for the homologous ketomethylene arginyl dipeptide surrogates required for the scissile position was developed. This modification confers subnanomolar affinity and proteolytic resistance. The most potent thrombin inhibitor was IId with K_i = 140 ± 20 pM. The standard of reference IIb (hirutonin-2) inhibited platelet aggregation mediated by thrombin and was a potent antithrombotic in vivo, comparable to hirudin. In order to further reduce the molecular weight of these inhibitors, the six intervening residues that function as a spacer were replaced by variable ω-aminopentenoyl units. The exosite component was also reduced to seven amino acid residues. The result of these combined modifications only marginally affected enzyme affinity (K_i = 3.5 ± 1.8 nM, IIIb). Molecular modeling studies suggest that the binding mode in the S′ groove for the two series differs markedly since the backbone of the ω-aminopentenoyl units of IIIb is extended and lies within the crevice. The compatibility of a truncated exosite-directed ligand terminating with Leu61 can be explained by the spatial coincidence with the same side chain function located in position 64 of the native sequence. However, an extended conformation for this side chain permitting interaction with another enzyme region cannot be ruled out. These low molecular weight hirudin peptides could form the basis of a new generation of antithrombotics in view of their high potency, specificity, and proteolytic stability.

Experimental Section

Melting points were determined on a Buchi 510 melting point apparatus and are uncorrected. ^{1}H NMR spectra were carried out on a Brüker AM-500 spectrometer. Spectra were analyzed on a Brüker Aspect 3000 workstation. Chemical shifts are reported in ppm (δ) downfield from Me_4Si. Analytical HPLC experiments were performed on a Beckman LC equipped with two 114 M solvent delivery modules, variable wavelength detector, and Vydac C_{18} analytical column. IR spectra were recorded on a Philips PYE UNICAM SP-300 spectrophotometer. Mass spectral analyses were carried out on a SCIEX API III spectrometer equipped with an ionspray inlet source. Exact mass measurements were performed by Dr. O. Mamer of the McGill University Mass Spectroscopy unit. Experiments were performed on a VG analytical ZAB-HS spectrometer equipped with a digital PDP 11/24 minicomputer VG 11-250 data system. Amino acid analyses and peptide content were determined on a Beckman Model 6300 amino acid analyzer. Optical rotations were measured on a JASCO DIP-370 digital polarimeter. Elemental analyses were done by Canadian Microanalytical Laboratory, Delta, B.C. Canada.

N^{α}-Boc-N^{ω}-Tosylarginine N,O-Dimethylamide (2). BOP reagent (500 mg, 1.1 mmol) was added to a solution of N^{α}-Boc-N^{ω}-tosylarginine (428 mg, 1 mmol) in 30 mL of DMF, at 0 °C in an ice bath, containing triethylamine (0.4 mL, 3 mmol) and N,O-dimethylhydroxylamine hydrochloride (146 mg, 1.5 mmol). The pH of the reaction was monitored and periodically adjusted to 8–9 by addition of triethylamine. The reaction was stirred overnight at 4 °C after which the solvent was evaporated under high vacuum. The residue was dissolved in 50 mL of EtOAc and washed with water. The organic phase was extracted further with 5% $NaHCO_3$ (3×) and 1 N HCl (3×) and washed with water. The solvent was dried over anhydrous Na_2SO_4, filtered over Celite, and concentrated in vacuo. Addition of a small amount of hexane deposited a solid which was isolated by filtration and recrystallized from EtOH affording 370 mg (79% yield) of a white powder, mp 148–150 °C. Mass spectral analysis: m/z 472 $(M + H)^+$; $[\alpha]^{20}_D$ = −11.4° (c 0.34, MeOH); ^{1}H NMR (DMSO) δ 1.3 (s, 9 H, t-Boc), 1.45 (m, 4 H, $\beta,\gamma CH_2$), 2.3 (s, 3 H, CH_3 Ar), 3.1 (b(d), 2 H, J = 5.5 Hz, δCH_2), 3.1 (s, 3 H, NCH_3), 3.7 (s, 3 H, OCH_3), 4.3 (b, 1 H, αCH), 6.9 (d, 1 H, J = 8 Hz, NH), 7.5 (q, 4 H, Ar). Anal. ($C_{20}H_{33}N_5O_6S\cdot H_2O$) C, H, N: calcd 49.07, 7.20, 14.30; found, 49.48, 6.95, 13.90.

6-(*N*-Boc-Amino)-9-(3-tosylguanidino)-1-nonen-5-one (3b). To a solution of 600 mg (1.3 mmol) of the N,O-dimethyl-

hydroxamate in 25 mL of THF was added 10 equiv of a Grignard reagent prepared from 4-bromo-1-butene [Note on preparation: 312 mg of magnesium turnings (13 mmol) in 50 mL of anhydrous ether under argon was treated with 1.75 g of 4-bromo-1-butene via syringe pump at a rate to maintain a gentle reflux]. After consumption of the metal, the Grignard solution was transferred with a syringe under argon to the THF solution cooled to 0 °C. The reaction was allowed to come to room temperature and monitored by TLC which showed no starting material after 5 h. The reaction was cooled in an ice bath and quenched by the dropwise addition of a 5 M solution of NH_4Cl. The phases were separated, and the organic phase was washed with 1 N HCl and H_2O, dried over Na_2SO_4, and evaporated under vacuum. Chromatography over silica gel eluting with 3:1 EtOAc/hexane afforded a clear oil corresponding to the unsaturated ketone (450 mg, 75% yield): mass spectral anal. m/z 468 $(M + H)^+$; $[\alpha]^{20}_D = -10.2°$ (c 0.25, MeOH); ^1H NMR ($CDCl_3$) δ 1.3 (s, 9 H, *t*-Boc), 1.6 (m, 4 H, $\beta,\gamma CH_2$), 2.0 (m, CH_2, $COCH_2CH_2$), 2.3 (s, 3 H, CH_3Ar), 2.4 (m, 2 H, $COCH_2$), 3.1 (d(b), 2 H, δCH_2N), 4.2 (b, 1 H, αCH), 5.0 (m, 2 H, $CH{=}CH_2$), 5.4 (d, 1 H, NH), 5.8 (m, 1 H, $CH{=}CH_2$), 6.1 (b, guanidino), 7.5 (q, 4 H, Ar).

7-(*N*-Boc-Amino)-10-(3-tosylguanidino)-1-decen-6-one (3c). Compound **3c** was synthesized analogous to **3b** except that the Grignard reagent obtained from 5-bromo-1-pentene was used. A thick oil that resisted crystallization was obtained after chromatography (70% yield): mass spectral anal. m/z 482 $(M + H)^+$; $[\alpha]^{20}_D = -10.7°$ (c 0.33, MeOH); ^1H NMR ($CDCl_3$) δ 1.3 (s, 9 H, *t*-Boc), 1.8–1.4 (m, 6 H), 2.0 (q, 2 H, CH_2CH), 2.3 (s, 3 H, CH_3Ar), 2.4 (m, 2 H, $COCH_2$), 3.2 (d(b), 2 H, CH_2N), 4.2 (b, 1 H, CHCO), 4.9 (m, 2 H, $CH{=}CH_2$), 5.4 (d, 1 H, NH amide), 5.5 (1 H, $CH{=}CH_2$), 6.2 (b, 3 H, guanidino), 7.5 (q, 4 H, Ar).

8-(*N*-Boc-Amino)-11-(3-tosylguanidino)-1-undecen-7-one (3d). This compound was synthesized analogous to **3b** except that the Grignard obtained from 6-bromo-1-hexene was used, affording a gum (70% yield): mass spectral anal. of the isolated oil gave m/z 496 $(M + H)^+$; $[\alpha]^{20}_D = -8.7°$ (c 0.47, MeOH); ^1H NMR ($CDCl_3$) δ 1.3 (s, 9 H, *t*-Boc), 1.8–1.4 (m, 8 H), 2.1 (m, 2 H, $CH_2CH{=}$), 2.3 (s, 3 H, CH_3 Ar), 2.4 (m, 2 H, $COCH_2$), 3.1 (d(b), 2 H, CH_2NH), 4.2 (b, 1 H, NHCH), 5.0 (d, 1 H, $CH{=}CH_2$), 5.5 (d, 1 H, NH), 5.8 (m, 1 H, $CH{=}CH_2$), 6.2 (b, 3 H, guanidino), 7.5 (q, 4 H, aromatic). Anal. ($C_{24}H_{38}N_4O_5S$) C, H, N: calcd 58.27, 7.74, 11.32; found 58.61, 7.90, 11.53.

5-(*N*-Boc-Amino)-4-oxo-8-(3-tosylguanidino)octanoic Acid (4b). An amount of 2.5 g (5.3 mmol) of the ketone **3b** was dissolved in 50 mL of acetonitrile and the solution was cooled in an ice bath. The solution was treated with 8 g (37.5 mmol) of sodium periodate in 50 mL of water. The mixture was treated with 100 mg of ruthenium chloride. After 1 h of vigorous stirring at room temperature, no starting material was observed by TLC. The mixture was diluted with 100 mL of H_2O and 100 mL of ether. The phases were separated, and the aqueous phase was extracted with 100-mL volumes of ether and 50 mL of ethyl acetate. The combined organic extracts were washed with H_2O, dried over Na_2SO_4, and evaporated to dryness under vacuum yielding 2 g of a yellow foam. The product was purified by column flash chromatography using 1% acetic acid in EtOAc giving 1.5 g (58% yield) of a white foam: mass spectral anal. calcd for $C_{21}H_{32}N_4O_7S$ 484.1990, exact mass observed m/z 485.2071 $(M + H)^+$; $[\alpha]^{20}_D = -18°$ (c 0.5, MeOH). For spectral characterization, the title compound was converted to the methyl ester using CH_2N_2: ^1H NMR ($CDCl_3$) δ 1.4 (s, 9 H, *t*-Boc), 1.8–1.5 (b, 4 H, CH_2CH_2 side chain), 2.3 (t, 2 H, CH_2CO), 2.4 (s, 3 H, CH_3Ar), 2.5 (m, 2 H, $COCH_2$), 3.2 (d(b), 2 H, CH_2N), 3.7 (s, 3 H, $COOCH_3$), 4.2 (b, 1 H, NHCH), 5.5 (d, 1 H, NH), 7.5 (q, 4 H, aromatic).

6-(*N*-Boc-Amino)-5-oxo-9-(3-tosylguanidino)nonanoic Acid (4c). Compound **4c** was obtained by the Sharpless oxidation of **3c**: mass spectral anal. calcd for $C_{22}H_{34}N_4O_7S$ 498.2146, exact mass observed m/z 499.2225 $(M + H)^+$; $[\alpha]^{20}_D = -24.6°$ (c 0.26, MeOH). A sample was treated with diazomethane for spectral analysis: ^1H NMR ($CDCl_3$) δ 1.4 (s, 9 H, *t*-Boc), 1.8–1.5 (b, 4 H, CH_2CH_2 side chain), 1.85 (p, 2 H, $CH_2CH_2CH_2$), 2.3 (t, 2 H, CH_2COO), 2.4 (s, 3 H, CH_3Ar), 2.5 (m, 2 H, $COCH_2$), 3.2 (d(b), 2 H, CH_2NH), 3.7 (s, 3 H, $COOCH_3$), 4.2 (b, 1 H, NHCH), 5.5 (d, 1 H, NH), 7.5 (q, 4 H, aromatic).

7-(*N*-Boc-Amino)-6-oxo-10-(tosylguanidino)decanoic Acid (4d). Compound **4d** was obtained by Sharpless oxidation of **3d**: mass spectral anal. calcd for $C_{23}H_{36}N_4O_7S$ 512.2302, exact mass observed m/z 513.2383 $(M + H)^+$; $[\alpha]^{20}_D = -10.9°$ (c 0.38, MeOH). A sample was treated with diazomethane as above: ^1H NMR ($CDCl_3$) δ 1.4 (s, 9 H, *t*-Boc), 1.8–1.5 (m, 8 H), 2.3 (t, 2 H, CH_2COO), 2.4 (s, 3 H, CH_3Ar), 2.5 (m, 2 H, $COCH_2$), 3.2 (d(b), 2 H, CH_2NH), 3.65 (s, 3 H, OCH_3), 4.2 (t, 1 H, NHCH), 6.5 (b, 3 H, guanidino), 7.5 (q, 4 H, aromatic).

Ethyl (*S*)-4-[(*tert*-Butyloxycarbonyl)amino]-3-oxo-7-(3-tosylguanidino)heptanoate (Mixed Anhyride Method). Isobutyl chloroformate (0.35 mL, 2.5 mmol) was added dropwise over 15 min to a stirring solution of 1 g (2.3 mmol) of (*S*)-N^{α}-Boc-Arg(N^{ω}-Tos)OH and triethylamine (0.48 mL) in 15 mL of THF under argon at −20 °C. The mixture was stirred vigorously for 45 min, diluted with 15 mL of anhydrous ether, and filtered through a 1-μm membrane filter. The filtrate was stored at −20 °C for the subsequent reaction.

Meanwhile, a stirring solution of diisopropylamine (3.4 mL, 24 mmol) in 50 mL of anhydrous ether under argon at 0 °C was treated dropwise with 9.6 mL of a 2.5 M solution of *n*-butyllithium using a syringe pump. The reaction was stirred for an additional 30 min after complete addition. The solution was cooled to −78 °C and treated dropwise with 2.3 mL of freshly distilled EtOAc over 20 min. The yellow reaction mixture was stirred further for 30 min followed by the addition of 3.3 g (24 mmol) of powdered $ZnCl_2$. The mixture was allowed to stir vigorously for 40 min and treated all at once with the previously formed mixed anhydride. The heterogenous reaction was stirred for 4 h at −78 °C, overnight at −20 °C, and quenched with 5 M NH_4Cl. The phases were separated, and the aqueous phase was extracted further with ether. The combined organic extracts were washed with 1 N HCl, H_2O, and dried over Na_2SO_4. The solvent was stripped under vacuum, and the residual oil was purified by silica gel flash chromatography using the solvent system 3:1 EtOAc/hexane, providing 500 mg of a viscous oil (43% yield): mass spectral anal. calcd for $C_{22}H_{34}N_4O_7S$ 498.2146, exact mass observed m/z 499.2225 $(M + H)^+$; ^1H NMR ($CDCl_3$/DMSO-d_6) δ 1.2 (t, 3 H, CH_3CH_2O), 1.4 (s, 9 H, *t*-Boc), 1.5 (b, 4 H, CH_2CH_2 side chain), 2.4 (s, 3 H, CH_3Ar), 3.2 (b, 2 H, CH_2 side chain), 3.5 (dd, 2 H, $COCH_2CO$), 4.2 (q, 2 H, CH_3CH_2O), 4.3 (b, 1 H, NHCH), 5.4 (d, 1 H, NH), 7.4 (q, 4 H, aromatic).

***N*-[(*S*)-4-[(*tert*-Butyloxycarbonyl)amino]-3-oxo-7-(3-tosylguanidino)heptanoyl]glycine.** The mixed anhydride formed from 2 g (4.6 mmol) of N^{α}-Boc-Arg(Tos)OH and isobutyl chloroformate was reacted with the enolate of ethyl thioacetate previously treated with $ZnCl_2$ as described for **7a**. Careful workup afforded 1.8 g of the crude ethyl (*S*)-4-[(*tert*-butyloxycarbonyl)amino]-3-oxo-7-(3-tosylguanidino)thioheptanoate (**8b**) which was used directly in the next reaction due to the inherent instability of the thioester on silica gel.[31]

The crude β-keto thioester (1.8 g) was dissolved in 20 mL of dichloromethane containing 2 equiv of triethylamine and 436 mg (1 equiv) of Gly-OMe·HCl. The mixture was then treated with cuprous iodide and stirred at room temperature. TLC analysis revealed that reaction was complete after 10 min. The mixture was treated with 50 mL of CH_2Cl_2 and 1 N HCl and filtered. The filtrate was washed with H_2O, dried over Na_2SO_4, and evaporated under high vacuum. The residue was chromatographed on silica gel eluting with 10:1 EtOAc/MeOH, affording 800 mg of a foam (32% yield from Boc-Arg(Tos)OH): mass spectral anal. calcd for $C_{23}H_{35}N_5O_8S$ 541.2204, exact mass observed m/z 564.2106 $(M + Na)^+$.

A solution of the adduct in 20 mL of 50% dioxane/H_2O was treated with 1 equiv of 1 N NaOH and stirred vigorously. The saponification was instantaneous affording 600 mg of the acid upon workup: ^1H NMR ($CDCl_3$/DMSO-d_6) δ 1.4 (s, 9 H, *t*-Boc), 1.6–1.4 (m, 4 H, CH_2CH_2 side chain), 2.4 (s, 3 H, CH_3 Ar), 3.1 (b, 2 H, CH_2NH), 3.5 (m, 2 H, $COCH_2CO$), 3.8 (b, 2 H, αCH_2Gly), 4.1 (b, 1 H, NHCH), 5.8 (b, 1 H, NH), 6.5 (b, 2 H, guanidino), 7.4 (q, 4 H, tosyl).

***trans*-β-Hydromuconic Acid Dimethyl Ester.** An amount of 22 g (153 mmol) of *trans*-β-hydromuconic acid was dissolved in 200 mL of benzene containing 500 mg of *p*-toluenesulfonic acid and 100 mL of methanol. The solution was heated in an oil bath at reflux for 6 h and treated with 100 mL of water. The phases were separated, and the organic layer was extracted further with 5% $NaHCO_3$ and H_2O. The organic phase was dried over Na_2SO_4

and evaporated under vacuum affording a clear oil which was purified by vacuum distillation (83–84 °C, 0.5 mmHg) to give 20 g of the title compound (77% yield).

***trans*-β-Hydromuconic Acid Monomethyl Ester.** An amount of 5 g (27.5 mmol) of the dimethyl ester was suspended with gentle mechanical stirring in 100 mL of a solution of 0.1 M KH_2PO_4 followed by addition of 20 mg of pig liver esterase. The pH of the solution was maintained between 7 and 7.5 by dropwise addition of a 1 M solution of LiOH. Following the consumption of 1 mol equiv of LiOH, the solution was treated with charcoal, stirred for 5 min, and filtered over Celite. The filtrate was extracted with ether, and the combined extracts were discarded. The aqueous phase was acidified with 6 N HCl and reextracted with ether. The combined organic extracts were dried over Na_2SO_4 and evaporated in vacuo. The residual oil was distilled under reduced pressure (105–110 °C, 0.5 Torr) affording 4 g (93% yield) of a colorless oil: ^1H NMR ($CDCl_3$) δ 3.1, 3.15 (dd, 4 H), 3.7 (s, 3 H, CH_3O), 5.7 (m, 2 H, CH=CH). Anal. ($C_7H_{10}O_4$) C, H.

4-(Methoxycarbonyl)-2-*trans*-didehydrobutyl Isocyanate. An amount of 1.2 g (7.6 mmol) of the monoester was dissolved in 25 mL of benzene under nitrogen and treated with 0.76 mL (8.7 mmol) of oxalyl chloride dropwise over 20 min. The solution was stirred for 4 h at room temperature, and the solvent was removed under vacuum. The residual oil was dissolved in 10 mL of acetone and added to a precooled solution (0 °C) of sodium azide (1 g) in 20 mL of 50% H_2O/acetone. After 30 min, the mixture was diluted with 50 mL of H_2O and extracted twice with 50-mL portions of toluene. The combined organic extracts were dried over Na_2SO_4 and filtered. The filtrate was heated in an oil bath at 80 °C until no further nitrogen evolution was observed. The solvent was cooled and evaporated under vacuum. The residual oil was distilled under reduced pressure (80–85 °C, 0.2 mm) affording 700 mg (58% yield) of the isocyanate which was used directly for the subsequent reaction, IR 2200 cm^{-1}. Anal. ($C_7H_9NO_3$) C, H, N: calcd 54.18, 5.85, 9.02; found 53.62, 5.72, 9.07.

5-[*N*-(*tert*-Butyloxycarbonyl)amino]-pent-*trans*-3-enoic Acid. An amount of 890 mg of *tert*-butyl alcohol (12.2 mmol) and 1 g (6.5 mmol) of the isocyanate were dissolved in 25 mL of toluene, and the solution was heated at reflux for 15 h. The solution was cooled, and the solvent was evaporated under vacuum. Distillation of the oil under reduced pressure afforded 1 g of the *tert*-butyl carbamate: bp 100–102, 0.2 mm (lit.[33] 111–112, 0.1 mm); ^1H NMR ($CDCl_3$) δ 1.4 (9 H, *t*-Boc), 3.0 (d, 2 H, CH_2CO), 3.6 (s, 3 H, OCH_3), 3.7 (b, 2 H, $NHCH_2$), 5.1 (b, 1 H, NH), 5.6 (m, 1 H, CH), 5.7 (m, 1 H, CH). Anal. ($C_{11}H_{19}NO_4$) C, H, N: calcd 57.62, 8.35, 6.11; found 56.60, 8.00, 6.03.

The preceeding ester was dissolved in 50 mL of 50% dioxane in water and treated with two equiv of NaOH. After 5 min the solution was diluted with 50 mL of H_2O and extracted with ether. The aqueous phase was made acidic with solid citric acid and extracted with 25-mL aliquots of EtOAc. The combined organic extracts were dried over Na_2SO_4, filtered, and evaporated under vacuum affording a thick gum: ^1H NMR ($CDCl_3$) δ 1.4 (s, 9 H, *t*-Boc), 3.1 (d, 2 H, J = 7 Hz, CH_2CO), 3.7 (b, 2 H, CH_2NH), 4.5 (b, 1 H, NH), 5.7–5.5 (m, 2 H, CH=CH). The acid was converted to the dicyclohexylammonium salt and crystallized from ether/hexane, mp 65–67 °C. Anal. ($C_{22}H_{40}N_2O_4 \cdot 2H_2O$) C, H, N: calcd H, N; 61.08, 10.25, 6.47; found 60.57, 9.05, 6.44.

[Ac-(D)Phe^{45},Pro^{46},Argψ[COCH$_2$]CH$_2$CO^{47}]Hirudin$^{45-65}$, Hirutonin-2, IIb. An amount of 1 g of (*tert*-butyloxycarbonyl)-Gln (phenylacetamido)methyl resin (Applied Biosystems; 0.64 mmol/g) was carried through 18 automatic cycles of coupling and deprotection. Coupling used 2.5 mequiv of protected amino acid mediated by DCC and *N*-hydroxybenzotriazole. Deprotection was mediated by 50% TFA in CH_2Cl_2.

The fully protected peptide resin was treated with 1 mL of dimethyl sulfide and treated with 7 mL of anhydrous hydrogen fluoride at −5 °C for 60 min. Excess HF was removed under a stream of N_2, and the residual mass was extracted with ether and filtered. The resin was extracted three times with glacial acetic acid and water, followed by lyophilization. The lyophilized crude peptide was purified to homogeneity by reverse-phase chromatography on an octadecyl silica glass column (2.5 × 30 cm, 15 Å Vydac, 40 psi) using a linear gradient of the solvent system consisting of (A) 500 mL of 0.1% TFA/H_2O and (B) 1 L of 60% acetonitrile/H_2O containing 0.1% TFA. The fractions were analyzed by analytical HPLC at 210 nm. Those corresponding to greater than 95% purity were pooled and lyophilized affording 500 mg of pure peptide. Amino acid analysis indicated: Asp (2.98), Ser (0.79), Glu (6.43), Gly (1.00), Ile (0.98), Leu (1.04), Tyr (0.97), Phe (2.00), His (1.00), Pro (1.87). The peptide showed a pseudomolecular ion corresponding to 2548.6 $(M + H)^+$.

[Ac-(D)Phe^{45},Pro^{46},Argψ(COCH$_2$)CH$_2$CH$_2$CO^{47,48}]Hirudin$^{45-65}$, Hirutonin-3, IIc. This compound was synthesized analogous to the procedure described for IIb except for 6-(Boc-amino)-5-oxo-9-(3-tosylguanidino)nonanoic acid which was used as the residue corresponding to positions 47–48. Amino acid analysis gave the following distribution: Asp (3.20), Ser (0.86), Glu (6.60), Gly (0.85), Ile (1.00), Leu (1.06), Tyr (0.86), Phe (1.84), His (0.88), Pro (2.10). The peptide showed a pseudomolecular ion corresponding to 2562.4 $(M + H)^+$.

[Ac-(D)Phe^{45},Pro^{46},Argψ(COCH$_2$)CH$_2$CH$_2$CH$_2$CO^{47,48}]Hirudin$^{45-65}$, (Hirutonin-4), IId. This compound was synthesized analogous to the procedure described for IIb except for 7-(Boc-amino)-6-oxo-10-(3-tosylguanidino)decanoic acid which was used as the residue corresponding to positions 47–48. Amino acid analysis gave the following distribution: Asp (3.15), Ser (0.84), Glu (6.84), Gly (1.00), Ile (1.04), Leu (1.26), Tyr (0.99), Phe (2.12), His (1.00), Pro (1.55). The peptide showed a pseudomolecular ion corresponding to 2576.3 $(M + H)^+$.

[Ac-(D)-Phe^{45},Pro^{46},Argψ(COCH$_2$)CO^{47,48},Gly^{49}]Hirudin$^{45-65}$, (Hirutonin-1), IIa. Peptide IIa was synthesized as described for IIb except for *N*-[(*S*)-4-[(*tert*-butyloxycarbonyl)amino]-3-oxo-(3-tosylguanidino)heptanoyl]glycine which was used as the residue corresponding to positions 47, 48, and 49. Amino acid analysis gave the following distribution: Asp (3.05), Ser (0.89), Glu (5.45), Gly (1.88), Ile (1.03), Leu (1.05), Tyr (1.05), Phe (1.79), His (0.93), Pro (1.95). The peptide showed a pseudomolecular ion corresponding to 2464.8 $(M + H)^+$, calcd 2463.3.

Synthesis of Truncated Peptides Having Synthetic Spacer Units (IIIa–c). These peptides were synthesized and purified essentially as described for IIb and its homologs with minor modifications. The solid phase synthesis began with (*tert*-butyloxycarbonyl)-Leu (phenylacetamido)methyl polystyrene resin (0.64 mmol/g). Side-chain deprotections following Asp55 were performed with 50% TFA in CH_2Cl_2 containing 10% ethyl methyl sulfide. Amino acid analysis and mass spectral characterization gave the following profile: IIIa, Asp (1.00), Glu (1.07), Ile (0.94), Leu (1.00), Phe (1.82), Pro (3.29); m/z = 1453, calcd 1452.4. IIIb, Asp (1.00), Glu (1.08), Ile (0.96), Leu (1.01), Phe (1.91), Pro (3.48); m/z = 1550.2, calcd 1548.5. IIIc, Asp (1.00), Glu (1.06), Ile (0.93), Leu (0.98), Phe (1.88), Pro (3.64); m/z = 1647.4, calcd 1644.6.

In Vitro Assay of Enzyme Inhibition. Amidolytic assays for the reported inhibitors were carried out at 25 °C in 0.1 M Tris-HCl buffer, pH 7.8, containing 0.1 M NaCl and 0.1% polyethylene glycol (PEG 6000). Human α-thrombin (300 units, 3080 units/mg, single band by SDS-PAGE) and the fluorescent substrate Tos-Gly-Pro-Arg-amc (K_m = 3.8 μM[14]) were purchased from Sigma Chemical Co., St. Louis, MO. Variable concentrations of substrate (ranging between 2.5 and 20 μM) dissolved in running buffer containing 5% DMSO and peptide inhibitor were mixed and adjusted to a volume of 3 mL in polypropylene cuvettes. The hydrolytic reactions were initiated by addition of 10 μL (30 pM) of a stock solution, 5 units/mL, of α-thrombin. Initial velocities were recorded on a Cary 2000 spectrophotometer operating in the fluorescence mode in the ratio (λ_{ex} = 383, λ_{em} = 455 nm). Fluorescence intensities were calibrated with known concentrations of 7-amino-4-methylcoumarin. Data for the rate of Amc release were analyzed using a nonlinear regression program RNLIN in the IMSL library[43] on a micro VAX 3500 computer. Data points were fitted to the eq 1 for competitive enzyme inhibition.[44] The

$$v = V_{max}S/K_m(1 + I/K_i) + S \quad (1)$$

selectivity for the active site of thrombin was examined in parallel sets of experiments using the substrates S-2222 (trypsin); S-2586

(43) IMSL Library Reference Manual, 1990, 9th ed.; version 1.0, IMSL, Houston, TX.
(44) Segel, I. H. *Enzyme Kinetics*; John Wiley: New York; Chapt. 3, 1975.

MeO-Suc-Arg-Pro-Tyr-pNA·HCl (chymotrypsin); S-2251 H-D-Val-Leu-Lys-pNA·2HCl (plasmin); and S-2765 N^{α}-Cbz-D-Arg-Gly-Arg-pNA·2HCl (factor Xa). These experiments used substrates and enzymes purchased from Kabi-Diagnostica (Pharmacia LKB GmbH, Freiburg, FRG).

In Vitro Plasma Stability of the Peptides. An amount of 600 μg of peptide was mixed with 250 μL of reconstituted normal human plasma, 250 μL of thromboplastin (Sigma), 600 μg of calcium chloride, and 50 mM $NaHPO_4$ buffer pH 7.8 adjusted to a final volume of 900 μL. The mixture was incubated at 37 °C and 100-μL aliquots were removed at designated time intervals. The individual aliquots were treated with 20 μL of 10% trichloroacetic acid and centrifuged for 10 min on an Eppendorf Model 5415C benchtop centrifuge. The supernatant was injected on a Vydac C_{18} analytical column and chromatographed by standard elution procedure (10%ACN/0.1%TFA in H_2O to 0.1% TFA in ACN).

Antithrombotic Activity of Hirutonin-2 in the Rat Arteriovenous Shunt Model. Rats anesthetized with urethane were fixed in a supine position on a temperature-controlled heating plate. The right carotid artery and the left jugular vein were catheterized with short polyethylene catheters (Portex, PE50). The catheters were filled with physiological saline solution and clamped. The two ends of the catheters were connected with a 2-cm glass capillary (internal diameter 1 mm) acting as a thrombogenic surface. Five minutes after intravenous administration of the test compound or its saline control, the clamps occluding the arteriovenous shunt were opened. Blood flowing through the shunt leads to a rapid rise in temperature of the glass capillary from room temperature to body temperature. The temperature change served as an indicator for the patency of the shunt. The temperature was measured by means of a NiCrNi-thermocouple.[45,46] The dose of compound required to cause a 15-min prolongation in patency of the shunt (ED_{15}) was recorded.

Platelet Aggregation. Platelet rich plasma (PRP) was prepared by centrifuging (180*g*, 8 min) normal citrated human plasma from healthy volunteers who had not taken medication for at least 2 weeks prior. The final platelet count was adjusted to 3×10^8 cells/mL with platelet poor plasma (PPP) obtained by centrifugation for 10 min at 1000*g*. Platelet aggregation was measured on a Bio/Data PAP-4 aggregometer. A volume of 225 μL of PRP and 150 μL of buffer (0.05 M Tris, 0.1 M NaCl, 0.1% PEG pH 7.8) or inhibitor were mixed and incubated at 37 °C for 3 min. A volume of 25 μL of α-thrombin (0.4 units/400 μL) was added and light transmission was recorded.

Molecular Modeling. The bimolecular models of IIb–thrombin and IIIb–thrombin were constructed by a modification of the procedure applied to the complex previously obtained for thrombin and I using the molecular modeling package of Quanta (version 3.0).[33,47] Conformational searches were performed using the program BatchMin[48] (version 3.1). The program Charmm[49] (version 21.1) was used for energy minimization and molecular dynamics simulations. All calculations were performed on an Iris 4D/280 (Silicon Graphics Inc.).

For the construction of the IIb–thrombin complex, the P_1' Pro residue was mutated to Gly using the *molecular modeling* submenu of Quanta. Using the *molecular editor* submenu, the NH group of Gly was changed to CH_2, and the carbon type was reset to CHE2 (in the polar hydrogen force field). A new residue topological file (RTF) was built for Argψ($COCH_2$)Gly. The resulting IIb–thrombin structure was energy minimized using the polar hydrogen force field and the ABNR (Adopted Basis Newton-Raphson) minimizer algorithm of Charmm. Except for the Argψ($COCH_2$)Gly dipeptidyl unit, all other coordinates of thrombin and IIb were restrained with a harmonic force constant of 20 kcal/mol. A 10-Å cutoff and a distance-dependent dielectric function ($\epsilon = 2r$) were used. The minimization was considered complete when an rms gradient of <0.1 kcal/Å was obtained.

The construction of the IIIb–thrombin model involved two operations. In the first, the oxobutylene scissile insert was built similar to its lower homolog (vide supra) and the spacer sequence (Gln[49]-Ser-His-Asn-Asp-Gly[54]) was replaced by two aminopentenoyl units ($NHCH_2CH{=}CHCH_2CO$). This was achieved by replacing the native amino acid sequence (49–54) by four Gly residues and converting the C=O and NH of the first and second glycine residue to CH while resetting the atom types to CUA. The second operation was the deletion of residues 62–65 from IIb and performing the mutations E58P and E61L using the *molecular modeling* submenu of Quanta. The two-aminopentenoyl spacer unit was subjected to energy minimization while restraining the remaining IIIb–thrombin coordinates.

To investigate the conformational role of the P_1' oxobutylene component of IIIb, a conformational search by high temperature molecular dynamics was conducted. This procedure involved all atoms of the IIIb–thrombin complex. All enzyme coordinates were fixed while the inhibitor residues 45–65 and 55–61, and NH, CA, and the side-chain atoms of Arg47 were constrained by harmonic constants. The temperature was increased from 0 to 1000 K during 3-ps dynamics simulation with 0.001-ps time steps. After 5-ps equilibration, 10-ps simulation was performed with data collection every 0.1 ps. The resulting conformers were subjected to energy minimization using the same constraints as the dynamics simulation.

To determine the conformation of the C-terminal Leu61 residue of the truncated peptide within the thrombin exosite, eight Monte Carlo multiple-minimum searches[50] were performed using BatchMin and the Amber force field.[51] The solvation energy[52] was included in the total energy and the dihedral angles ψ of Pro60, and Φ and χ_1 of Leu61 were included in the search. The substructure used consisted of inhibitor residues 59–61 and enzyme residues 34, 36, 65, 76, and 82–84. Atoms within 4 Å of these residues were also loaded but with a distance-dependent potential anchoring. Each run had 150 Monte Carlo steps and generated conformers that were subjected to 100-step conjugate gradient minimizations, setting the energy window to 200 kJ/mol.

Stochastic boundary molecular dynamics[53,54] were introduced to simulate the interactions between the thrombin exosite and the right hand side of IIIb. Charmm and the polar hydrogen force field were used in this computation. An approximately spherical *reaction* region of the IIIb–thrombin model having a radius of 10 Å was used, together with the low energy conformer previously determined in the conformational search. The position of the Ile59 Cβ was used as the center of reference in the sphere, and the reaction region was surrounded by a 2-Å *buffer*. The sphere included residues D-F-E-P-I-P-L of IIIb and the thrombin loops

(45) Ashida, S.; Sakuma, K.; Aiko, Y. Antithrombotic effects of ticlopidine, acetylsalicylic acid and dipyridamone in vascular shunt model in rats. *Thromb. Res.* **1980**, *17*, 663–671.
(46) Shand, R. A.; Smith, J. R.; Wallis, R. B. Expression of the platelet procoagulant activity in vivo in thrombus formation in an extracorporeal shunt in the rat. *Thromb. Res.* **1984**, *36*, 223–232.
(47) Quanta version 3.0, 1990, Polygen Corp., 200 Fifth Ave., Waltham, MA 02154.
(48) Mohamadi, F.; Richards, N. G. J.; Guida, W. C.; Liskamp, R.; Lipton, M.; Caufield, C.; Chang, G.; Hendrickson, T.; Still, W. C. MacroModel—An Integrated Software System for Modeling Organic and Bioorganic Molecules Using Molecular Mechanics. *J. Comput. Chem.* **1990**, *11*, 440–467.
(49) Brooks, B. R.; Bruccoleri, R. E.; Olafson, B. D.; States, D. J.; Swaminathan, S.; Karplus, M. CHARMM: A Program for Macromolecular Energy Minimization and Dynamics Calculations. *J. Comput. Chem.* **1983**, *4*, 187–217.
(50) Chang, G.; Guida, W. C.; Still, W. C. An Internal Coordinate Monte Carlo Method for Searching Conformational Space. *J. Am. Chem. Soc.* **1989**, *111*, 4379–4386.
(51) Weiner, S. J.; Kollman, P. A.; Case, D. A.; Singh, U. C.; Ghio, C.; Alagona, G.; Profeta, S.; Weiner, P. A New Force Field for Molecular Mechanical Simulation of Nucleic Acids and Proteins. *J. Am. Chem. Soc.* **1984**, *106*, 765–784.
(52) Still, W. C.; Temczyk, A.; Hawley, R. C.; Hendrickson, T. Semianalytical Treatment of Solvation for Molecular Mechanics and Dynamics. *J. Am. Chem. Soc.* **1990**, *112*, 6127–6129.
(53) Brunger, A. T.; Huber, R.; Karplus, M. Trypsinogen-Trypsin Transition: A Molecular Dynamics Study of Induced Conformational Change in the Activation Domain. *Biochemistry* **1987**, *26*, 5153–5162.
(54) Brooks, C. L.; Karplus, M. Solvent Effects on Protein Motion and Protein Effects on Solvent Motion Dynamics of the Active Site Region of Lysozyme. *J. Mol. Biol.* **1980**, *208*, 159–181.

31–41 and 62–85. The space inside the reaction and buffer zones was filled with water by overlaying a previously-equilibrated box of TIP3P water molecules. Water molecules within 2.6 Å of any protein atom were removed from the system. A constant dielectric function of 1 was employed, and a cutoff distance of 10 Å for nonbonded interactions was used for both the van der Waals and the electrostatic terms. The temperature was maintained at 300 ± 5 K by coupling all non-hydrogen atoms in the buffer zone to a Langevin bath. The SHAKE constraint algorithm was employed to keep bonds involving hydrogen atoms fixed at their equilibrium position. After an 8000-step equilibration of the water structure in the presence of the fixed protein and a 20000-step equilibration of water and protein structures, a second TIP3P water overlay was applied to fill voids in the solvent. The 100000-step dynamics simulation was carried out with data collection every 50 steps. For a dynamics trajectory of N frames the rms fluctuation (Δrms) of an atom is given by $\Delta\text{rms} = ((1/N)\sum_{i=1}|r - (r)_{av}|^2)^{1/2}$.

Acknowledgment. The authors are indebted to Dr. J. D'angelo of l'Hopital Maisonneuve Rosemont for expert technical assistance in performing platelet aggregation assays.

Determination of the Absolute Configuration of the Active Amlodipine Enantiomer as (−)-*S*: A Correction

Siegfried Goldmann,* Jürgen Stoltefuss, and Liborius Born

Bayer AG, Pharma Research Center, Postfach 10 17 09, 5600 Wuppertal 1, Germany. *Received January 10, 1992*

The active (−) enantiomer of amlodipine was originally reported to have *R* configuration. This does not concur with other 1,4-dihydropyridines with known absolute configuration. This configuration has now been determined by X-ray structural analysis using (1*S*)-camphanic acid and (*S*)-2-methoxy-2-phenylethanol as chiral probes. Both determinations gave the *S* configuration for the amlodipine (−) enantiomer with the greater Ca-antagonistic activity.

Ca-antagonistic 1,4-dihydropyridines of type 1 with asymmetric ester substitution are chiral, and the enantiomers naturally differ in their pharmacological activity. A number of derivatives of 1 with known absolute configuration demonstrate that the more active enantiomer is the one that—with the aryl residue represented as shown—has the larger ester on the left-hand side[1] (usually the *S* configuration).

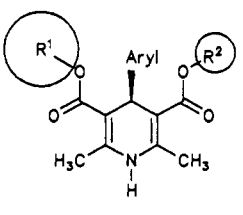

1

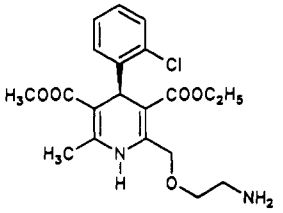

R-2

more potent enantiomer ($R^1 > R^2$)

A major exception seemed to be amlodipine **2**, whose *R* enantiomer (*R*-**2**) was described as pharmacologically more active.[2] Basic substitution in the 2-position with the possibility of additional hydrogen bridges was postulated as an explanation for this behavior. However, findings that correlate better with the *S* configuration for the active (−) enantiomer of amlodipine led us to doubt whether the reported configuration was correct, particularly since the X-ray structure from which the *R* configuration had been inferred had not been published.[2] Accordingly, we repeated the investigation of the absolute configuration.

Correlation with (1*S*)-Camphanic Acid (Sheme I)

Using (−)-(1*S*)-camphanic acid chloride (**3**), racemic amlodipine (**2**) was converted into the diastereomeric

Scheme I

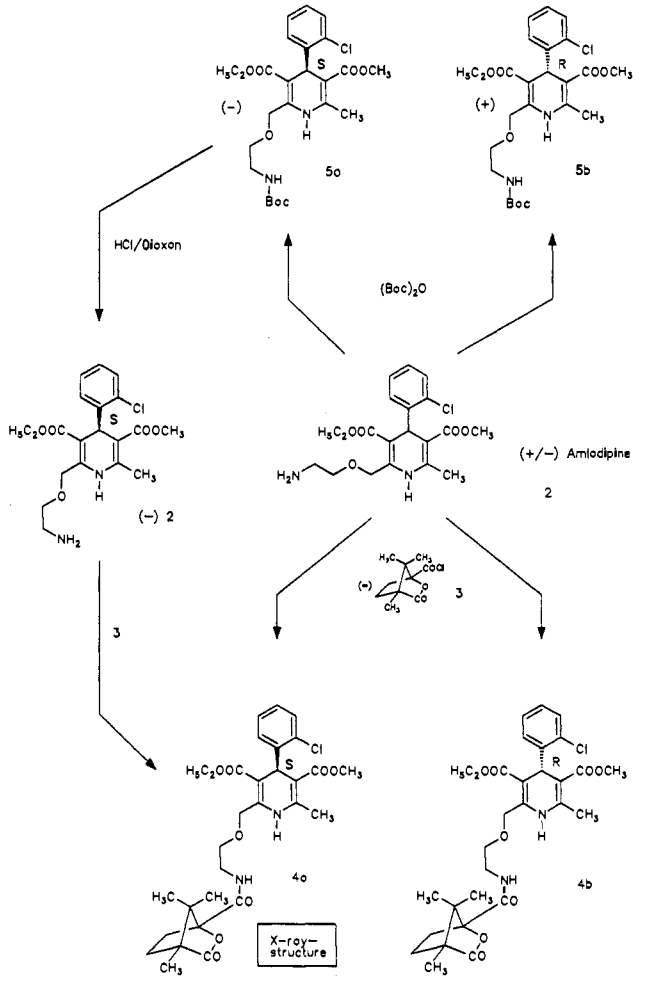

amides **4a** and **4b**, which are very easy to separate matographically. By crystallizing **4a** from DMF/water, single crystals suitable for X-ray structural analysis were obtained. The X-ray structure of **4a** gave the *S* configuration at the dihydropyridine carbon (Figure 1).

The agreement of the configuration of **4a** with the active (−) enantiomer of amlodipine ((−)-**2**) was shown by inde-

(1) Goldmann, S.; Stoltefuss, J. 1,4-Dihydropyridines: Effects of Chirality and Conformation on the Calcium Antagonist and Calcium Agonist Activities, *Angew. Chem. Int. Ed. Engl.* **1991**, *30*, 1559–1578.

(2) Arrowsmith, J. E.; Campbell, S. F.; Cross, P. E.; Stubbs, J. K.; Burges, R. A.; Gardiner, D. G.; Blackburn, K. J. Long-Acting Dihydropyridine Calcium Antagonists. 1,2-Alkoxymethyl Derivatives Incorporating Basic Substituents. *J. Med. Chem.* **1986**, *29*, 1696–1702.

0022-2623/92/1835-3341$03.00/0